The role of molecular packing on the UV-visible optical properties of $[Re_2Cl_2(CO)_6$4,5-$(Me_3Si)_2$pyridazine]

P. Spearman *[a], S. Tavazzi [a], L. Silvestri [a,b], A. Burini [a], A. Borghesi [a], P. Mercandelli [c], M. Panigati [d], G. D'Alfonso [d], A. Sironi [c], L. De Cola [e]

[a] Università degli Studi di Milano Bicocca, Dipartimento di Scienza dei Materiali, Via Cozzi 53, I-20125 Milano, Italy
[b] School of EE&T, University of New South Wales, Sydney, NSW 2052, Australia
[c] Università degli Studi di Milano, Dipartimento di Chimica Strutturale e Stereochimica Inorganica Via Venezian 21, I-20133 Milano, Italy
[d] Università degli Studi di Milano, Dipartimento di Chimica Inorganica, Metallorganica e Analitica Via Venezian 21, I-20133 Milano, Italy
[e] Westfälische Wilhelms Universität Münster, Mendelstrasse, 7 48149 Münster,Germany
*peter.spearman@unimib.it

ABSTRACT

We report here on two stable polymorphs of the dinuclear complex $[Re_2(\mu\text{-}Cl)_2(CO)_6(\mu\text{-}4,5\text{-}(Me_3Si)_2$pyridazine)]. The compound–belongs to the recently reported class of dinuclear luminescent Re(I) complexes of general formula $[Re_2(\mu\text{-}Cl)_2(CO)_6(\mu\text{-}1,2\text{-}$diazine)]. In the solid state, the complex exhibits a unique combination of unusual properties: (i) concomitant formation of two highly luminescent polymorphs, and single crystal- to-single-crystal conversion of one form into the other, (ii) remarkable differences in the absorption properties of the two polymorphs due to different redistribution of oscillator strength among the different excitons, and (iii) remarkable differences among the emission properties. In particular, a higher emission quantum yield was found in the solid state than in solution (measured to be 0.52 and 0.56 for the two polymorphs, almost one order of magnitude higher than that of the molecule in solution).

Interest in luminescent materials able to efficiently emit in the solid state is continuously growing, because in most applications the dyes are used as solid films. Although rigid environments are expected to freeze roto-vibrational relaxation pathways, luminescence efficiency often decreases in the solid state with respect to liquid solution due to concentration quenching, affecting both organic and organometallic emitters. However, an increasing number of molecular-based emitters exhibit enhanced solid state emission. Apart from the importance of bulky substituents in reducing concentration quenching effects, other intra- or inter-molecular phenomena have been invoked as well, such as conformational changes, π-π stacking, hydrogen bonds, or J-aggregates, which cause rearrangements of the energy levels and population. In these two polymorphs the enhancement of the emission with respect to the solution is most likely due to the restricted rotation of the Me_3Si groups in the crystals, providing an interesting example of aggregation-induced emission effect (AIE).

To provide more insight into the optical properties of the two polymorphs, we present a combined computational and experimental study in the framework of crystal optics in the aim to explore the role of molecular packing on the UV-visible absorption properties of the two known polymorphs of $[Re_2(\mu\text{-}Cl)_2(CO)_6(\mu\text{-}4,5\text{-}(Me_3Si)_2$pyridazine)].

Keywords: polymorphism, intermolecular interaction, rhenium complex, molecular excitons, organometallic emitters

1. INTRODUCTION

The interest towards high luminescent transition-metal complexes is continuously growing because of their general versatility, chemical stability and ability to capture and emit light efficiently. In solid state devices, the organization of the molecule plays a crucial role in determining the photo-physical properties insofar as the absorption of light and the color and the emission quantum yield are concerned. A well-known consequence of aggregation is the quenching of fluorescence due to charge-transfer, energy-transfer, or via formation of H-type aggregates. In the case of transition-metal complexes, a reduction of the photoluminescence quantum yield accompanying aggregation, is attributed to several processes: concentration-quenching by triplet-triplet annihilation or creation of low-lying excited states or nonradiative paths mediated by intermolecular interactions such as π-π stacking, metal-metal interaction, hydrogen bonds and dipole-dipole interactions[1]. However, a new class of materials shows an enhancement of the emission in the aggregate state – or aggregation-induced emission[3]. A recent addition to this class is the dinuclear rhenium(I) complex $[Re_2(\mu\text{-}Cl)2(CO)_6(\mu\text{-}4,5\text{-}(Me_3Si)_2pyridazine)]$ (**1**), reported by some of us (Figure 1).[4], which shows stronger emission in the crystalline phase than in solution.This complex belongs to the family of neutral Re(I) complexes with general formula $[Re_2(\mu\text{-}X)_2(CO)_6(\mu\text{-}1,2\text{- diazine})]$, where X is halogen. Some of them have recently gained interest for their intense yellow/green emission, occurring from triplet metal-to-ligand charge transfer states showing a modulation effect of the diazine substituent on wavelengths, lifetimes, and quantum yields of the emission.[5] In particular, complex **1** shows an intriguing combination of properties: formation of two highly luminescent polymorphs, irreversible single-crystal-to-single-crystal transformation from one polymorph into the other, and a remarkable difference in the emission quantum yield of the two polymorphs in the solid state with respect to the solution (up to 0.56 vs 0.06 for the solution). This latter effect has been tentatively attributed to the restricted rotation, occurring in the crystalline phase, of the Me_3Si groups, which are involved in the LUMO level.[4] However, these restricted roto-vibrational motions cannot explain the different colors observed for the two polymorphs, both in the absorption and in the emission spectra. The maximum of the absorption band detected at lowest energy in the polycrystalline form was measured at 3.15 eV for one polymorph and 3.35 eV for the other one.[4] A similar behavior is recorded for the emission spectra since the two species emit in the green (2.32 eV) and in the orange (2.18 eV).[4] To find a possible explanation, our first focus was on the understanding of the role of intermolecular interactions. We noticed that, for the single molecule, the singlet electronic transitions at lowest energies are relatively weak and consequently, strong excitonic interactions leading to large shifts in excited states energies in the two polymorphs were not expected.[6] On these grounds we have investigated the role of higher-energy transitions to explain the differences in the optical properties between the two polymorphs. Here, we present a combined study of the structure, anisotropy, and crystal optics, which demonstrates that the differences in the absorption properties are ascribed to the different molecular packing and consequent re-distributions of excitonic transitions.

2. EXPERIMENTAL SECTION

2.1 Synthesis

The rhenium complex **1** was synthesized by refluxing in toluene solution the $[ReCl(CO)_5]$ with the appropriate amount of the 4,5-bis(trimethyl-silyl)pyridazine ligand, as previously reported.[4] A scheme of the synthetic route and of the molecule is reported in Fig. 1

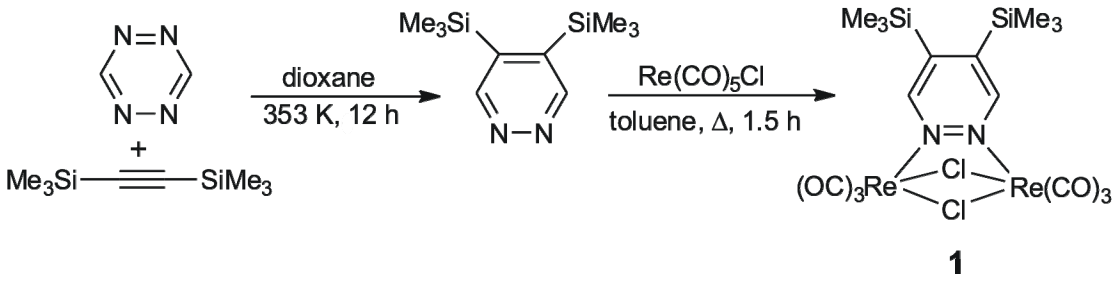

Figure 1 Synthetic scheme of $Re_2(\mu\text{-}Cl)_2(CO)_6(\mu\text{-}4,5\text{-}(Me_3Si)2pyridazine)$ (1). [7]

2.2 Crystallization of different polymorphs

During the crystallization process, complex (**1**) can produce the concomitant formation of two polymorphs in the solid state, denoted as orange phase (**1O**) and yellow phase (**1Y**).[4] For example, crystallization by slow diffusion of *n*-hexane into a concentrated CH_2Cl_2 solution of **1** at room temperature afforded crystals of both phases. Because concomitant polymorphs are nearly energetically equivalent structures, kinetic rather than thermodynamic contributions offer the best tool to obtain each phase alone. By modifying the crystallization rate it was thus possible to separately isolate the two forms. The two forms were obtained separately by modifying the crystallization rate: fast evaporation from CH_2Cl_2 solution afforded pure **1Y**, whilst very slow crystallization (by CH_2Cl_2/*n*-hexane diffusion at 253 K) gave pure **1O** (or at worst mixtures much richer in **1O** than **1Y**). An approach to increase the crystal size of **1O** adopted a very slow solvent evaporation of a saturated solution of the complex in methane trichloride. A crystal sample and the solution were left in a sample vial that has a very small perforated cap. Together with the desired crystal, small crystals of the other polymorph also formed, and so the crystal was removed before complete evaporation of the solvent. In a contrasting way, it was possible to increase the size of the **1Y** phase with fast solvent evaporation of a saturated solution of methane dichloride. Crystals were also grown by the floating-drop technique (FD),[9] dissolving 5-6 mg of sublimated product in 3 mL of xylene. The solution was filtered (pore size: 0.2 μm), placed on the surface of deionized water and kept in air during solvent evaporation. With this method, both polymorphs were obtained. Another method to obtain **1Y** crystals was by irreversible **1O** → **1Y** phase transition that was induced by thermally treating **1O** crystals using a Linkam THMS600 Heating Stage.As reported in ref. [4] **1O** crystalizes in the orthorhombic space group $Pna2_1$ (No. 33, a = 21.509(2) Å, b = 6.355(2) Å, c = 36.997(2) Å at room temperature) with two independent molecules in the asymmetric unit and eight molecules in the unit cell, while **1Y** crystalizes in the monoclinic space group $I2/a$ (No. 15, a = 11.204(2) Å, b = 12.782(2) Å, c = 18.751(2), β = 101.90(2)° (at room temperature) with half a molecule in the asymmetric unit (the molecule lying on a C_2 axis) and four molecules in the unit cell.

2.3 Instrumentation and analysis performed

Single crystals of the two phases were selected under crossed polarizations using an optical polarizing transmission microscope Olympus SZX12. Images of the crystal samples were also taken under an Olympus BX51 fluorescence microscope. Polarized absorbance measurements in the UV-visible spectral range were taken at normal incidence using a Perkin-Elmer Lambda 900 spectrometer equipped with Glan-Taylor calcite polarizers.

3. RESULTS AND DISCUSSION

3.1 1O and 1Y polymorphs: structure, shape

1O grows as a platelet in which the most developed forms correspond to the *ab* face. Figure 2 shows few images of a **1O** crystal taken under the transmission microscope with either parallel polarized and analyzer (left images) or crossed polarized and analyzer (right images). We notice that the complete extinction of the transmitted light in the latter case indicates that the crystal is single. Moreover, the direction of maximum length of the sample

and the orthogonal direction are directions of extinction and hence, correspond to principal axes of the system[10,11].

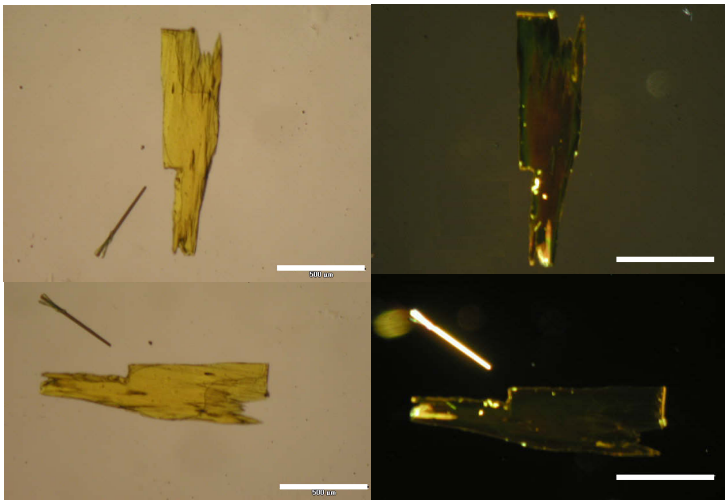

Figure 2 Images of a **1O** sample under the polarizing transmission microscope. The bars correspond to 0.5 mm. The images on the left (right) were taken with parallel (crossed) polarized and analyzer.

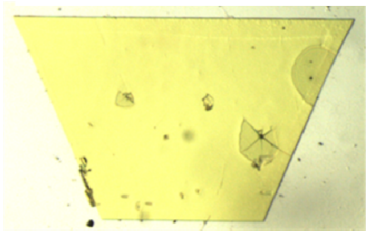

Figure 3. Image of a **1Y** crystal under the transmission microscope. This sample was grown by floating drop.

Independently of the growth method we adopted, **1O** typically showed a similar habit with, *ab* being the most prominent face. **1Y** can also be grown by different methods, with typical morphology consisting of a rhombic prism {011} as shown in Fig. 3. In these crystals the *ab* face is expected to be either absent or only slightly developed.[7] For this reason, we preferred to study the optical properties of **1Y** crystals obtained by inducing the irreversible **1O** → **1Y** phase transition by progressively heating **1O** in a nitrogen atmosphere. Figure 4 shows two images taken on the same sample under the transmission microscope before and after the temperature-induced phase transition (left panels), together with two images taken on the same portion of the same sample under the fluorescence microscope during the phase transition (central panels). In the latter case, the colors recorded by the camera are slightly different with respect to those observed by the naked eye due to experimental artifacts. As determined by variable temperature single-crystal X-ray diffraction experiments,[4] the **1O** → **1Y** phase transition leaves almost unchanged the direction of the crystallographic axes of the two phases. As a consequence, the exposed face of the **1Y** platelets obtained by phase transition corresponds to the *ab* face and we can also assume their *a* and b axes to be almost parallel to the corresponding axes of the starting **1O** phase. The molecular packing for the two polymorphs is shown in the right panels of Fig. 4.

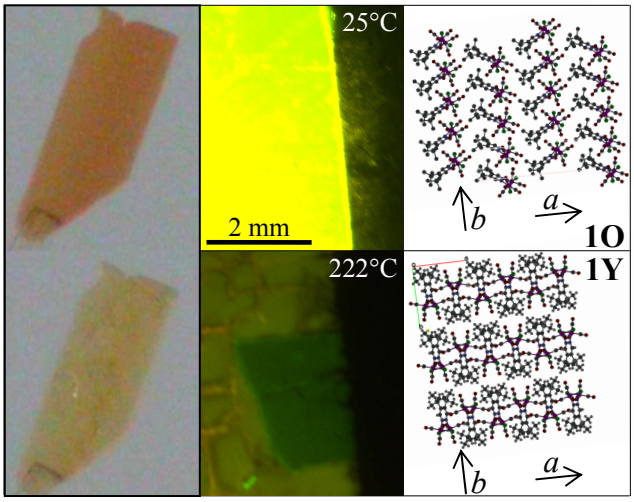

Figure 4. . Images taken on the same sample under the transmission microscope before and after the temperature-induced phase transition (left panels), together with two images taken on the same portion of another sample under the fluorescence microscope during the phase transition (central panels). In the latter case, the colors recorded by the camera are slightly different with respect to those observed by the naked eye due to experimental artifacts. The molecular packing for the two polymorphs is shown in the right panels.

3.2 1O and 1Y polymorphs: UV-visible absorption

Figure 5 shows the UV-visible absorption spectra measured at normal incidence on the accessible face (*ab*) of (a) **1O** and (b) **1Y** obtained by **1O** → **1Y** phase-transition. In both cases, the two spectra correspond to the two orthogonal directions of polarization of the incident light along the *a* ad *b* unit-cell axes. For the **1O** crystal, the *b*-polarized spectrum shows a band centered at about 3.2 eV. The center of the *a*-polarized band can be tentatively deduced to be at about 3.2-3.3 eV. Despite saturation, the ratio between the intensities of the two orthogonally-polarized bands can be deduced to be between 2 and 3. For the **1Y** crystals, a relatively strong band is observed for one polarization and it too is widely affected by saturation, but its center can be tentatively deduced to be at about 3.4-3.5 eV. For the other polarization, a weak band is detected centered at about 3.2 eV.

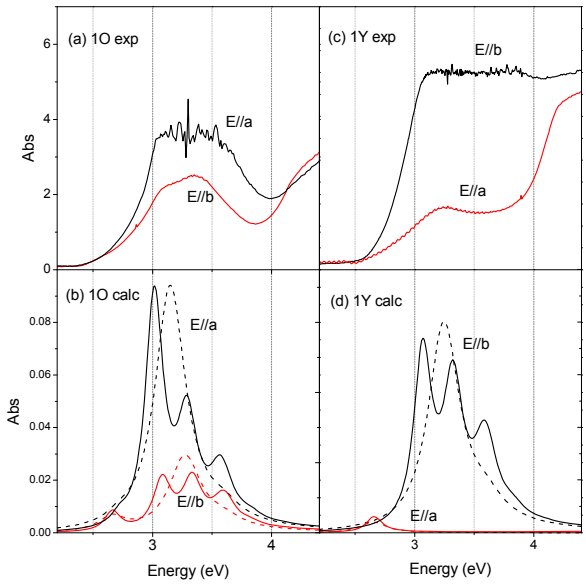

Figure 5. Normal-incidence absorption spectra measured with orthogonal polarizations on (a) a 1O crystal, (c) a 1Y crystal obtained by **1O** → **1Y** phase transition and simulated for (b) **1O** and (d) **1Y** with *ab* exposed face for either *a* or *b* polarization. The simulated spectra assume either purely electronic transitions (full line) or using vibronic coupling regime with effective frequency 0.26 eV and Huang-Rhys parameter equal to 1.

For the understanding of the optical properties of the solids, the electronic optical transitions of the isolated molecule have been computed with Gaussian03.[12] The calculations were carried out on the optimized geometry of the molecule, which possesses C_2 symmetry. The singlet excitation energies were computed by means of time-dependent density functional calculations. The parameter-free hybrid functional PBE0 was employed along with the standard valence double-ξ polarized basis set 6-31G(d,p) for C, H, Cl, N, and O. For Re the Stuttgart–Dresden effective core potentials were employed along with the corresponding valence triple-ξ basis set. Results are reported in Table I for the singlets at lowest energy. The most intense transitions of the single molecule are the 6th, which is polarized along the long molecular axis *L*, and the 3rd, which is mostly along the *M* axis. The *L*, *M*, and *N* axes are defined as the inertial axes of the molecule, where *L* is the longest one, *N* is the shortest one.

Table 1. Computed singlet electronic transitions of the molecule

	Transition dipole moment (Debye)			Osc. strength	Energy (eV)
	N	*M*	*L*		
1	0	0	0.035842	0	2.4509
2	-0.17718	-0.00102	0	0.0003	2.6279
3	0.00331	2.63326	0	0.0699	2.6606
4	0.156333	-0.02517	0	0.0003	3.0055
5	0	0	-0.01347	0	3.0764
6	0	0	-4.46629	0.2434	3.2177
7	-0.24429	-0.01042	0	0.0008	3.5402
8	0	0	1.315485	0.0237	3.6076
9	0	0	-0.00534	0	3.7127
10	-0.02923	-0.28979	0	0.0013	4.0768

In the crystal, each molecular electronic transition is predicted to give rise to several excitonic transitions, depending on the number of molecules per unit cell.[2]

We can express crystal excitonic states in terms of delocalized wavefunctions and excitonic bands can be found by diagonalizing the corresponding resonance-interaction matrix[2] In the present case, excitonic interactions inside the crystal were approximated to be interactions between point-dipoles located at the center of mass of each molecule and the resonance-interaction matrix has been computed for an infinite crystal using Ewald's method.[2] Coupling between different molecular transitions has been included, which causes some redistribution of the excitonic intensities between all the states involved, although the effect is relatively small and for brevity, we do not discuss it. Also, any gas-to-crystal shift has been neglected. Leading from the calculation of the exciton energies and their strengths, the material dielectric tensor of each polymorph was built from the relation[2]

$$\hat{\varepsilon}_{ij}(E) = \varepsilon_\infty \delta_{ij} + \frac{2}{\varepsilon_0 V} \sum_n \left(\frac{(d_n)_i (d_n)_j E_n}{E_n^2 - E^2 - i\gamma E} \right) \quad (1)$$

where d_n is the calculated dipole moment in the direction of the n-th transition, ε_0 is the vacuum permittivity, V is the volume of the unit cell, $\gamma(E)=0.1E$ is a damping factor, ε_∞ is a background term which was taken equal to 3.6[8,11], and E_n is the calculated energy for the n-th excitonic transition. From the material dielectric tensor, a transfer matrix algebra can be used to describe the propagation of a monochromatic plane wave through an anisotropic medium with a given thickness to extract its absorbance spectrum.[14] Two types of simulation were performed: in the first case, only the purely electronic transitions (extracted from Table 1) were considered, whilst in a second case a vibrational mode was added to the 6th molecular transition. We included an effective vibrational mode with frequency 2100 cm^{-1} which is based on an average of a cluster of frequencies we found in the calculated IR spectrum. The adiabatic transition energy E_{00} was calculated by subtracting the excited state relaxation energy $\Delta E_{FC} = S\nu$ from the vertical transition energy, where S is the Huang-Rhys parameter and ν is the coupled vibrational mode[15]. We assumed the vertical transition to be the maximum energy found in the spectrum, corresponding to the centroid of a Franck-Condon progression with Huang Rhys parameter equal to 1.

The simulated curves for the **1O** crystal (*ab* exposed face) are reported in Figure 5c and those for the yellow polymorph **1Y** in Figure 5d. In the **1O** case, each molecular electronic transition gives rise to eight excitonic bands. They must be polarized along the unit-cell axes, as expected for orthorhombic crystals.[7,10,11] At the center of the Brillouin zone, out of eight states, two are dark, two are polarized along the crystal *a* axis, two along *b* and two along *c*. When considering that the exposed face of the **1O** crystals is the *ab* face, two orthogonally-polarized main transitions in the same spectral range are expected originating mainly from the 6th molecular transition as seen in Fig 5(a) and in the simulation (panel c). The most intense band is the *a* polarized band with intensity ratio between the *a*- and *b*-polarized bands expected to be almost 3, in good agreement with the measured ratio.

The simulated spectra show the peculiar characteristics of the corresponding experimental spectra. In the case of the purely electronic approximation (dashed line), this energy is found equal to 3.19 eV, while the maximum in the vibronic regime is red-shifted approximately by one vibration energy (0.26 eV). There is evidence of some underlying structure in the experimental spectra for the two polarisations – especially in the *b*-polarisation spectrum, which is exposed more clearly in the simulated spectra. For the **1Y** polymorph, each molecular transition gives rise to four excitonic bands, which are either *b* or *ac* polarized, as expected for monoclinic crystals where *b* is the monoclinic axis.[11,13] Out of four excitonic states, three are dark. As far as the strongest molecular transition is concerned (6th, *L* polarized), the *L* molecular axes of the four molecules in the unit cell are all parallel to each other and parallel to the *b* axis (Fig. 6). For this reason, the allowed excitonic transition (8.93 D) of **1Y** is *b*-polarized. The 3rd molecular singlet comes from a *MN*-polarized molecular transition (mainly M-polarized) and is predicted to give a single relevant absorption peak, which is expected to be *ac*-polarized (mainly *c*-polarized, forming an angle of about 20° with the *c* axis). Indeed, the *M* and *N* molecular axes of all the four molecules in the unit cell are parallel to the *ac* plane.

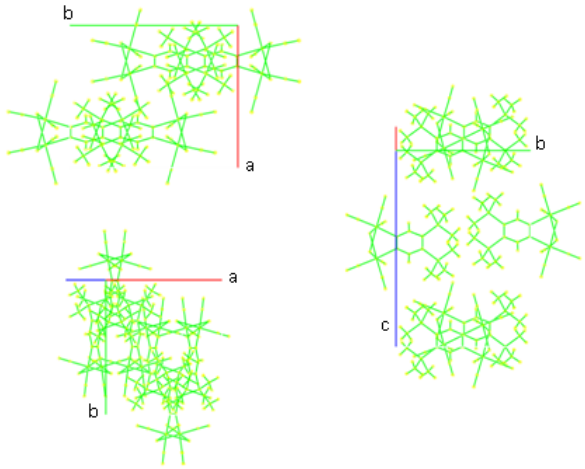

Figure 6. 1Y molecular packing.

Based on these considerations, at normal incidence on the *ab* exposed **1Y** face it is possible probing the *b*-polarized excitons and the projections along the *a* axis of the *ac*-polarized ones. However, the *ac*-polarized transition originating from the 3rd molecular singlet is negligible with respect to the strong *b*-polarized band originating from the 6th molecular singlet. Indeed, the measured spectra in Fig. 5c do not show any significant band at about 2.7 eV corresponding to the *ac* transition, while a strong band is observed in the *b*-polarized experimental spectrum, whose center has been tentatively deduced to be at about 3.4-3.5 eV. This band is mainly attributable to the *b* polarized excitonic state from the 6th molecular transition. We believe that the weaker band at about 3.2 eV in the measured *a*-polarized spectrum is a consequence of a slightly uncompleted phase-transition. Indeed, the *a* axis of the **1Y** crystal after the phase transition coincides with the *a* axis of the starting **1O** crystal (as already discussed) and a pronounced band is expected at about 3.2 eV for the *a*-polarized **1O** phase (see panels (a) and (c) of Fig. 5). The main features of the experimental curves are well reproduced in the simulated spectra, in particular the polarization and relative intensity of the optical bands.

Conclusions

From this experimental and computational study of the crystal structure, shape and optical properties of $Re_2(\mu\text{-}Cl)_2(CO)_6(\mu\text{-}4,5\text{-}(Me_3Si)_2pyridazine)$, the relevant role of molecular packing in governing and tailoring the UV-visible properties are deduced. This study on the two polymorphs (**1O** and **1Y**) of this rhenium complex allowed the attribution of the observed UV-visible absorption bands, of their polarizations and intensities in the framework of the theory of molecular excitons. Experimental and calculated results are in good agreement. Molecular packing is the key-factor causing the main differences between the absorption properties of the two polymorphs since it induces different redistributions of oscillator strength among the possible excitons. In particular, we underline that the aggregation is H-like only for the **1Y** polymorph (concerning the 6th molecular electronic transition). The different effects of vibronic coupling for the two polymorphs have also been reported.

REFERENCES

[1] Baková, R.; Chergui, M.; Daniel, C.; Vlcek Jr, A.; Zális, S. *Coordin. Chem. Rev.* **2011**, *25*, 975.

[2] Davydov, A.S. *Theory of Molecular Excitons*, Plenum: New York, 1971.

[3] (a) Chen, J.; Xu, B.; Ouyang, X.; Tang, B.Z.; Cao, Y. *J. Phys. Chem A* **2004**, *108*,7522; (b) Xie, Z.; Yang, B.; Cheng, G.; Liu, L.; He, F.: Shen, F.; Ma, Y.; Liu, S. *Chem. Mater.* **2005**, *17*, 1287; (c) Yin, S.; Peng, Q.; Shuai, Z.; Fang, W.; Wang, Y.-H.; Luo, Y., *Phys. Rev. B* **2006**, *73*, 205409; (d) Peng, Q.; Yi, Y.; Shuai, Z.; Shao, J.; *J. Chem. Phys.* **2007**, *126* 11430

[4] Quartapelle Procopio E.; Mauro, M.; Panigati, M.; Donghi, D.; Mercandelli, P.; Sironi, A.; D'Alfonso, G.; De Cola, L. *J. Am. Chem.Soc.* **2010**, *132*, 14397.

[5] (a) Donghi, D.; D'Alfonso, G.; Mauro, M.; Panigati, M.; Mercandelli, P.; Sironi, A.; Mussini, P.; D'Alfonso, L. *Inorg. Chem.* **2008**, *28*, 4243; (b) Mauro, M.; Quartapelle Procopio, E.; Sun, Y.; Chien, C.H.; Donghi, D.; Panigati, M.; Mercandelli, P.; Mussini, P.; D'Alfonso, G.; De Cola, L. *Adv. Funct. Mater.* **2009**, *19*,2607.

[6] In ref. [4], the formation of H-aggregates was indeed ruled out on the ground of the large intermolecular distances and the relatively low oscillator strength of the molecular electronic transition at lowest energy.

[7] Tavazzi, S.; Silvestri, L.; Spearman, P.; Borghesi, A.; Mercandelli, P.; Panigati, M.; D'Alfonso, G.; Sironi, A.; Cola, L. D., *Crystal Growth & Design* **2011,** *12* (2), 742-749.

[8] Tavazzi, S.; Raimondo, L.; Silvestri, L.; Spearman, P.; Camposeo, A.; Polo, M.; Pisignano, D. *J. Chem. Phys.* **2008** *128*, 154709.

[9] Campione, M.; Ruggerone, R.; Tavazzi, S.; Moret, M. *J. Mater. Chem.* **2005**, *15*, 2437.

[10] Born, M. Wolf, E. *Principle of Optics*; Cambridge University Press: New York, 1999.

[11] (a) Tavazzi, S.; Borghesi, A.; Papagni, A.; Spearman, p.; Silvestri, l.; Yassar, A.; Camposeo, A.; Polo, m.; Pisignano, D. *Phys. Rev. B* **2007**, *75*, 245416; (b) Tavazzi, S.; Silvestri, L.; Campione, M.; Borghesi, A.; Papagni, A.; Spearman, P.; Yassar, A.; Camposeo, A.; Pisignano, D. *J. Appl. Phys.* **2007**, *102*, 023107.

[12] Frisch, M.J.; Trucks, G.W.; Schlegel, H.B.; Scuseria, G.E.; Robb, M.A.; Cheeseman, J.R.; Montgomery, J.A.Jr; Vreven, T.; Kudin, K.N.; Burant, J.C.; Millam, J.M.; Iyengar, S.S.; Tomasi, J.; Barone, V.; Mennucci, B.; Cossi, M.; Scalmani, G.; Rega, N.; Petersson, G.A.; Nakatsuji, H.; Hada,

M.; Ehara, M.; Toyota, K.; Fukuda, R.; Hasegawa, J.; Ishida, M.; Nakajima, T.; Honda, Y.; Kitao, O.; Nakai, H.; Klene, M.; Li, X.; Knox, J., Rabuck, A. D.; Raghavachari, K.; Foresman, J.B.; Ortiz, J.V.; Cui, Q.; Baboul, A.G.; Clifford, S.; Cioslowski, J.; Stefanov, B.B.; Liu G.; Liashenko, A.; Piskorz, P.; Komaromi, I.; Martin, R.L.; Hratchian, H.P.; Cross, J.B.; Bakken, V.; Adamo, C.; Jaramillo, J.; Gomperts, R.; Stratmann, R.E.; Yazyev, O.; Austin, A.J. ; Cammi, R.; Pomelli, C.; Ochterski, J.W.; Ayala, P.Y.; Morokuma, K.; Voth, P. Salvador, G.A.; Dannenberg, J.J.; Zakrzewski, V.; Dapprich, S.; Daniels, A.D.; Strain, M.C. ; Farkas, O.; MalickFox, D.J.; Keith, T.; Al-Laham, M.A.; Peng, C.Y.; Nanayakkara, A.; Challacombe, M.; Gill, P.M.W.; Johnson, B.; Chen, W.; Wong, M.W.; Gonzalez, C.; Pople J.A. *Gaussian 03*, *Revision D.02*, Gaussian, Inc., Wallingford, CT, **2004**.

[13] (a) Spearman, P.; Borghesi, A.; Campione, M. Laicini, M.; Moret, M:, Tavazzi, S: *J. Chem. Phys.* **2005**, *122*, 014706; (b) Laicini, M.; Spearman, P.; Tavazzi, S.; Borghesi, A. *Phys. Rev. B* **2005**, *71*, 045212; (c) Tavazzi, S.; Campione, M.; Laicini, M.; Raimondo, L.; Spearman, P.; Borghesi, A. *J. Chem. Phys.* **2006**, *124*, 194701; (d) Raimondo, L.; Laicini, M.; Spearman, P.; Tavazzi, S.; Borghesi, A. *J. Chem. Phys.* **2006**, *125*, 024702; (e) Tavazzi, S.; Miozzo, L.; Silvestri, L.; Mora, S.; Spearman, P.; Moret, M.; Rizzato, S.; Braga, D.; Diagne Diaw, A.K.; Gningue-Sall, D.; Aaron, J.-J.; Yassar, A. *Cryst. Growth & Design* **2010**, *10*, 2342; (f) Girlando, A.; Ianelli, S.; Bilotti, I.; Brillante, A:; Della Valle, R.G.; Venuti, E.; Campione, M.; Mora, S.; Silvestri, L.; Spearman, P.; Tavazzi, S. *Cryst. Growth & Design* **2010**, *10*, 2752; (g) Tavazzi, S.; Mora, S.; Alessandrini, L.; Silvestri, L. *J. Chem. Phys.* **2011**, *134*, 034707.

[14] Schubert, M. *Phys. Rev. B* **1996**, *53*, 4265.

[15] Gierschner. J, Mack H-G, Luer L., and Oelkrug D.; J. Chem. Phys. 116, 8596 (2002); B□ssler H. and Schweitzer B; Acc. Chem. Res. **1999,** 32, 173-182